Efficient Global Optimization Under Conditions of Noise and Uncertainty – A Multi-Model Multi-Grid Windowing Approach

Vicente J. Romero
Sandia National Laboratories[1]

1. Abstract

Incomplete convergence in numerical simulation such as computational physics simulations and/or Monte Carlo simulations can enter into the calculation of the objective function in an optimization problem, producing noise, bias, and topographical inaccuracy in the objective function. These affect accuracy and convergence rate in the optimization problem. This paper is concerned with global searching of a diverse parameter space, graduating to accelerated local convergence to a (hopefully) global optimum, in a framework that acknowledges convergence uncertainty and manages model resolution to efficiently reduce uncertainty in the final optimum. In its own right, the global-to-local optimization engine employed here (devised for noise tolerance) performs better than other classical and contemporary optimization approaches tried individually and in combination on the "industrial" test problem to be presented.

2. Keywords

Global, Local, Search, Optimization, Structured Sampling, Convergence, Model Resolution, Uncertainty

3. Introduction, Background, and Nature of the Problem

In several recent optimization applications at Sandia, small-scale stochastic noise arising from finite numerics in computational physics simulations (see *e.g.* [1]-[3]) has made the use of classical gradient-based nonlinear programming (NLP) local optimization algorithms inefficient and in some cases ineffective. As demonstrated in [1] and [4], added noise from other numerical operations that account for uncertainty in the optimization problem amplifies the need to develop noise-tolerant optimization strategies. As explained in [1], noise, bias, and topographical inaccuracy in the objective function are related in a complex and nondirect (sometimes stochastic) way to resolution of the underlying models and sampling procedures. *By understanding how noise, bias, and topographical inaccuracy in the objective function vary with model resolution the optimization procedure can be managed for an optimal balance of efficiency, accuracy, and reliability.*

The nature of the matter is exemplified by Figure 1a which, for various degrees of temporal resolution of the thermal model used to compute the objective function in the test problem [5], plots 1-D parameter studies of objective function behavior versus discrete increments in one of the design parameters (fire radius *r*) in the optimization problem. As shown in [1] similar properties exist with respect to the other design variable in the problem. The designations LOOSE, XSTRICT, etc. of the various curves in the figure correspond to various settings (see Table 1) of the iterative convergence tolerance parameters EPSIT1 and EPSIT2 that control adaptive time-marching in the thermal solver QTRAN[6]. A convergence study in [1] shows that the simulations on which the smooth XSTRICT curve in Figure 1a is based are effectively fully converged with respect to timestep. As convergence tolerances are relaxed, however, noise and bias appear in the objective function as the other curves demonstrate. Noise and bias arise from finite numerics in computational simulations, *e.g.* truncation of series solutions, noninfinitesimal spatial and temporal discretization, incomplete convergence in iterative procedures, insufficient (unconverged) sampling, machine roundoff, etc.

The spacing of the data points in Figure 1a is 0.005 inch. This is a much larger "sampling scale" than the finite-difference step sizes of approximately 0.001 inch used in the final optimization runs in [5]. Since the frequency and severity of noise increases with decreasing sampling scale (see [1]), the noise experienced by the conjugate-gradient optimizer in [5] was probably much worse than that displayed in Figure 1a. Nevertheless, the optimizer was able to navigate the design space to the optimal (minimum) point using XSTRICT function evaluations (FEVs). However, for the more noisy objective functions the path to the minimum is less direct (more zigzagged, decreasing the efficiency of the process) and in some cases the noise is debilitating, trapping the optimizer in a numerical minimum that the algorithm mistakes for the local physical minimum.

When sampled at a large enough scale the objective functions associated with the various model tolerances have nearly the same "macro" shape as Figure 1b shows. The "macro curve" representations are quadratic curves passing through the left-most, center, and right-most points of the data in Figure 1a. Despite being based on variously converged simulations the quadratic representations all exhibit similar relative topography or shape. *Since it is **relative** topography that is important in optimization, the vertical bias in the curves is immaterial.* This is fortunate because vertical location of such curves depends not only on numerical parameters in the model, but even more strongly on physical parameters such as material properties, boundary condition coefficients, geometry parameters, etc. Since large uncertainty exists in many of these parameters, large uncertainty likewise exists in the vertical location of the objective function, but the *relative* topography changes much more slowly with uncertainty in the driving parameters (see *e.g.* [4] and [7]). As documented in [1], the minima of the macro curves occur at *r* values that differ from each other by only a few tenths of a percent and differ by an average of half a percent from the "target" value of *r* (=1.62 in. at the minimum of the XSTRICT curve in Figure 1a). Furthermore, achieving such accuracy can be very inexpensive. Even the XLOOSE macro curve, which is based on three XLOOSE simulations each 1/20 the cost of a comparable XSTRICT simulation (see Table 1 –CPU times

---

1. This work was supported by the United States Department of Energy under Contract DE-AL04-94AL8500.

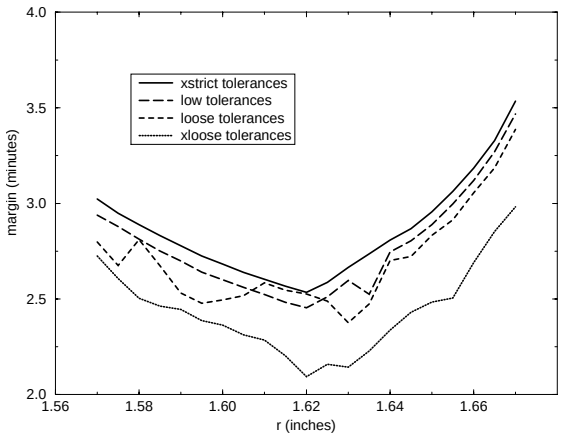

Figure 1a Numerical noise in objective function for various temporal convergence tolerances in the thermal model. Parameter study is along *r* for *x*=0.782 in., revealing the optimum identified in [5].

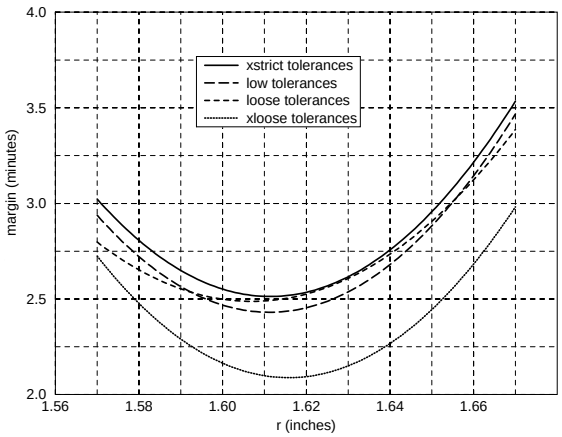

Figure 1b Quadratic "macro curves" based on values at the endpoints and midpoints of the curves in Figure 1a.

were obtained on a dedicated 200-Mhz SUN ULTRA2 workstation), yields an optimal design value that is within half a percent of the target optimum. Thus, in optimization *large potential savings reside in the weakened requirements (relative rather than absolute accuracy) on the underlying simulation models.*

Obviously the objective function must be sampled on a large enough scale that the amplitude of the local numerical noise does not seriously undermine the ability of the optimizer to correctly interpret the local physical topography in the problem. Samping scale, however, is also constrained by the desired resolution in the optimization problem (the smaller the sampling scale the better the resolution in the design space). Therefore, the local physical topography and the desired resolution (sampling scale) in the optimization problem determine the level of noise that can be tolerated, which puts demands on the resolution of the underlying computational models. The difficulty is that noise level must be determined experimentally and does not correlate dependably with model resolution. For example, the XLOOSE curve in Figure 1a seems to have noise of less amplitude than the LOOSE curve. In fact, it is shown in [1] that this trend continues, where progressively *less* temporally resolved X.5XLOOSE and XXLOOSE simulations yield progressively *smoother* such curves even though the relative topographical accuracy begins to degrade.

Under the competing goals of accuracy and affordability the optimal model is the one with lowest resolution (therefore the least expensive) that can produce noise within the level ultimately dictated by the desired resolution in the optimization problem, but which also delivers "sufficient" relative topographical accuracy. The optimal model, however, is not knowable *a priori*, it must be determined by running models of appropriately different resolution at critical points or phases of the optimization process. *The challenge of contemporary optimization is to, in a robust, efficient, and practical manner, use multiple model resolutions to identify and eliminate inaccuracy and noise problems that could defray the optimization process (where the causative factors can vary greatly with problem type and even over the design space of a single problem).* Active model management implies decreased uncertainty and increased robustness in the optimization process, but can also result in large cost savings relative to running a single model successfully over the spectrum from start to finish in a global optimization problem.

Table 1 Per-Timestep QTRAN[6] Convergence Tolerance Settings and Associated CPU Time Requirements at {*r*,*x*} = {1.6204 in., 0.78205 in.} = optima found in [5] at XSTRICT tolerances

tolerance level	EPSIT1 tolerance	EPSIT2 tolerance	CPU time (min.)	% of XSTRICT time	number of timesteps	% of XSTRICT # of timesteps
XSTRICT	$1x10^{-4}$	$1x10^{-6}$	72.68	100.0%	984	100.0%
LOW	$1x10^{+0}$	$1x10^{-2}$	10.28	14.1%	171	17.4%
LOOSE	$1x10^{+1}$	$1x10^{-1}$	4.31	5.9%	96	9.8%
XLOOSE	$1x10^{+2}$	$1x10^{-0}$	3.4	4.7%	90	9.1%
X.5XLOOSE	$1x10^{+3}$	$1x10^{+1}$	2.9	4.0%	90	9.1%
XXLOOSE	$1x10^{+4}$	$1x10^{+2}$	2.0	2.8%	90	9.1%

Regarding optimization engines, classical gradient-based methods are strictly for local optimization. Noise-tolerance can be attained with large enough perturbations in finite-differencing operations, but unavoidable inaccuracy in finite-differenced derivatives contributes to multi-dimensional zigzag inefficiency. Efficiency has been improved with more contemporary algorithms such as coordinate pattern search (CPS) for local optimization and genetic algorithms (GA) for global/local stochastic searching (see [3]). Hybrid combinations of NLP, CPS, and GA approaches with different levels of model refinement (different QTRAN tolerance levels) have proven even more effective. However, these sophisticated techniques have various free parameters such as sampling scale, sampling strategy, retention, crossover, and mutation rates, and population sizes and number of generations, etc. that are best resolved by a combination of expert opinion and experimentation with the problem at hand. Certainly, much research still remains in determining robust and suitable metrics for selecting sampling scale for the problem at hand and then optimal matching model resolution, and in determining when to switch from one model and/or optimization algorithm to the next when conditions change upon advancing through the design space and/or increasing the resolution requirements in the optimization problem.

In contrast, the optimization scheme advocated in this paper is based on a rather simple structured sampling paradigm[8] (originally devised for tolerance to noise) that happens to fit nicely into a model-management framework by: 1) naturally providing prominent decision points in the global-to-local optimization process that are convenient pauses for assessing model-resolution effects and changing models if necessary; and 2) eliminating or fixing several free parameters in the overall problem in an effort to increase manageability therefore confidence and executability of the process. The approach relies on structured sampling combined with a globally C^0 continuous, piecewise smooth local representation of objective function topography with finite-element polynomial interpolation functions of linear to quadratic order (see *e.g.* [8]). In the global/local sampling phases the intent of the sampling plan is to maximally reduce ignorance (lack of global/local knowledge within the design space) with each new sample, while simultaneously maximizing leveragability in anticipated future rounds of sampling. The sampling plan dictates the sampling scale in the problem autonomously, progressively refining the scale according to logic-based rules described in [9]. The global-to-local optimization scheme is found (see [9]) to be significantly more efficient than any of the classical or contemporary optimization approaches already tried on the “industrial” test problem [5], whether used singly or in combination with multiple models or not.

4. Demonstration of Efficient Uncertainty-Reducing Framework: Global Optimization Phase

Figure 2 shows a 2-D parameter space of fire radius *r* and center location *x* that is to be searched to find the combination of parameters that discriminately heats a hypothetical weapon safing device so as to minimize its safing ability as explained in [5]. Before embarking on the optimization process an assessment must be made of the convergence behavior of the underlying numerical model and the implications for the pending process. A convergence study at the middle of the design space (presented in [1]) reveals that oscillatory convergence occurs up through the various tolerance levels up to the asymptotically converged XSTRICT level and that X.5XLOOSE tolerances mark a distinct “knee” in the convergence curve. Oscillatory convergence indicates that the objective function will probably be noisy in the local optimization phase of the problem. At this initial (global) stage noise is not an issue but topographical inaccuracy is; using a model with excessivley loose convergence tolerances can identify incorrect “regions of promise” to be interrogated later in the local optimization phase. It is impossible to tell *a priori* the lowest (thus least expensive) model resolution that will produce sufficiently accurate topographical information to yield to the same regions of promise that the asymptotically converged model would. However, lacking more to go on, the X.5XLOOSE model at the knee of the curve is picked as the “minimal model”. (The appropriateness of this choice will be ascertained later by the framework.)

Beginning the global searching phase of the process, the ×‘s in the parameter space in Figure 2 represent the two lowest *diverse* global minima of a biquadratic response surface fit to objective function values calculated with X.5XLOOSE model tolerances for the parameter pairs indicated by the nine Lattice Sampling[8] Level 3 square markers in the figure. (The ✳'s in the figure indicate analogous minima based on simulations employing XXLOOSE tolerances, which are determined for research purposes here but would not normally be sought.) The minima are obtained by analyzing 10201 response surface values evaluated on a 101x101 grid overlying the design space. Thus, resolution in the design space at this global phase is 1/100 or 1% of the respective parameter ranges. These “grid-point” optima are therefore subject to a likely uncertainty of +/- 0.5% in the design space. The circled optima of each set are the primary (lower) minima.

Figure 3 shows updated optima for the piecewise smooth Lattice Sampling Level 4 global response surface corresponding to the indicated discretization of the design space into one central biquadratic “quad”[rilateral] element and four surrounding linear-to-quadratic transition “tri”[angle] elements. Only four new FEVs (at the triangular markers shown) are required to get to the Level 4 representation from the previous Level 3 representation. Both primary and secondary optima are seen to shift significantly from Level 3 to Level 4 resolutions of the design space. Figure 4 shows results for Lattice Sampling Level 5, where resolution of the objective function has been increased substantially by running the model at the 12 additional points indicated by the solid dots in the figure. A Level 5 representation utilizes four biquadratic quad elements that span the space as indicated. In going from the previous two levels to this level of refinement a major shift occurs in the locations of both primary and secondary optima. Figure 5 shows results for Lattice Level 6, where 16 additional samples at locations marked by the open circles in the figure have been added for a total of 41 now covering the design space. A piecewise smooth C^0 response surface consisting of five biquadratic quads, four quadratic tri’s, and four linear-to-quadratic transition tri’s presides. From Level 5 to Level 6 a major shift occurs in the location of the secondary optimum but a relatively small shift occurs in the location of the primary optimum (more on this later).

At this juncture consideration should be given to switching to the local optimization phase of the problem. In the present framework the global searching phase is intended to identify *regions* (not points) of design space having high potential

for containing the global optimum. Accordingly, progressive Lattice Sampling refinement need only be pursued until the locations of optima in the two most recent Lattice Sampling levels differ by 10-20% (as a percentage of full range of the design variables). The underlying issue is whether global topography is sufficiently resolved that local optimization can be "safely" pursued. If resources are fixed (not the case here) an earlier switching point might be selected in the desire to reserve enough resources for the local optimization phase. In any case, the burden of selecting a switching point is eased by the "quantized" nature of Lattice Sampling, which categorizes decision alternatives into quantified, separate, and prominent "chunks". For example, the question before us now is: Should global refinement be continued with Lattice Level 7, a regular 9x9 array of points over the design space that require 40 new FEVs thereby essentially doubling the number performed to this point, or can 40 such FEVs be used more profitably in local or semi-local refinement?

In considering this question, from Level 5 to Level 6 the coordinates of the primary minimum change by about -19% in *r* and -13% in *x* as percentages of the full ranges of the design variables (*i.e*. 5.3 in. in *r* and 5.9 in. in *x*). This meets the criterion recommended above for switching from global to local searching. However, the coordinates of the secondary minimum change by about 27% in *r* and the maximum of 100% in *x*. Obviously the location of the secondary minimum is not corroborated between Levels 5 and 6. In fact, through the other resolution levels the location of the secondary optimum also varies much more wildly than that of the primary optimum. Moreover, a different interpolation of the sample points of Lattice Level 6 can be obtained by shifting the interpolation pattern vertically or horizontally by one column or row of points. The resulting discretization of the design space into quadratic quads and tri's is depicted in Figure 6. The associated piecewise-continuous global response surface yields the primary and secondary minima denoted by the +'s in the figure. The two different interpolations yield absolute differences of 0.5% and 12.5% in *r* and *x* for the location of the primary minimum but respectively 17% and 40% for the secondary minimum. The relative instability of the predicted location of the secondary minimum raises doubt that a dominant secondary minimum exists in the problem. Indeed, by plotting the Level 6 response surface (Figure 7) it appears that a unique secondary minimum does not exist. Rather, a plane of roughly equal secondary minimums exists. Furthermore, the primary minimum appears to be vastly dominant, having an interpolated value of about -120.8 minutes versus 6.54 minutes for the next lowest diverse minimum. This is enough evidence to deem the primary optimum as the only viable optimum for further consideration. Thus, 40 FEVs would best be spent in pursuing this optimum locally rather than in another round of global refinement.

Before proceeding with local optimization the level of uncertainty in the location of the primary optimum must first be assessed and minimized. The interpolated values of the primary minima for Level 6 are -120.8 minutes for the Figure 5 interpolation and -29 minutes for the Figure 6 interpolation. This large disparity due to interpolation uncertainty alone suggests extreme, quickly varying topography in this region of the design space. Hence the objective function is expected to vary significantly over the nonnegligible separation distance between the two points, in which case one minimum would dominate the other. Accordingly, two FEVs are performed and indeed the X.5XLOOSE safety margin at the circled × in Figure 5 is about 9 minutes, while the global minimum at the circled + in Figure 6 is a much subordinate 23 minutes. A comparison against actual (not interpolated) objective function values at the existing 41 Lattice points verifies that the circled optimum in Figure 5 marks the lowest confirmed minimum in the design space. We contemplate a next phase of local refinement about this point in pursuit of the global minimum, but want to be reassured that the very inexpensive but temporally unconverged X.5XLOOSE model has not led us astray. Therefore a parameter study over model tolerance is run at this location similar to the one initially performed at the center of the design space. It is found (see [1]) that the XLOOSE model is the least expensive to provide at these two points an essentially constant bias from asymptotically converged XSTRICT results. Assuming that this trend (constant bias) holds reasonably well over the entire design space, the XLOOSE model will identify the same global optimum in the design space that the converged XSTRICT model would, at less than 1/20 the cost (*cf*. Table 1). Accordingly, a cost-efficient maximization of reliability in the global findings is attained by repeating the foregoing analysis with XLOOSE model tolerances. It happens that the results lie on the marked X.5XLOOSE primary and secondary optima in Figures 2-6 exactly, corroborating them to within the +/- 0.5% resolution uncertainty of the design-space grid.

Exact corroboration indicates that the approach taken is perhaps overly conservative and more costly than necessary. To check (this would not normally be done in anything but "research mode"), the process is repeated with XXLOOSE tolerances and the results are marked by the ✳'s in Figures 2 - 5. At all Lattice Levels the locations of the XXLOOSE secondary optima are considerably different from the corroborated results. However, the locations of the dominant primary minima are acceptably accurate. These results indicate that the approach taken is perhaps a bit conservative, but not overly so. This check lends support to the convention that the "minimal model" to start with in the global optimization phase is the one marking the "knee" in a convergence curve generated at the center of the global design space. This approach toward maximizing reliability of located optima can also be applied in the case of other types of resolution/ convergence uncertainties such as those associated with spatial discretization. Other sources of uncertainty due to variability and uncertainty of critical model parameters such as material properties, constituitive equation constants, boundary condition coefficients, *etc*. that can be treated as random variables are best handled with the complementary optimization-under-uncertainty framework applied in [4] and [7].

5. Demonstration of Efficient Uncertainty-Reducing Framework: Local Optimization Phase

In this framework a "dual-model" strategy is used in the local optimization phase primarily to reduce the chances of objective function noise leading the process astray, although topographical inaccuracy (if significant on such a small design-space scale) will also likely be detected and mitigated. The convergence study alluded to above suggested that the XLOOSE model is the minimal model for global accuracy. Certainly this model will be accurate over the much smaller

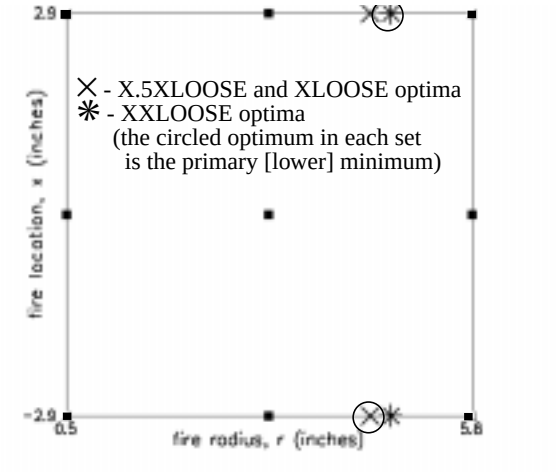

Figure 2 (Lattice Sampling Level 3)

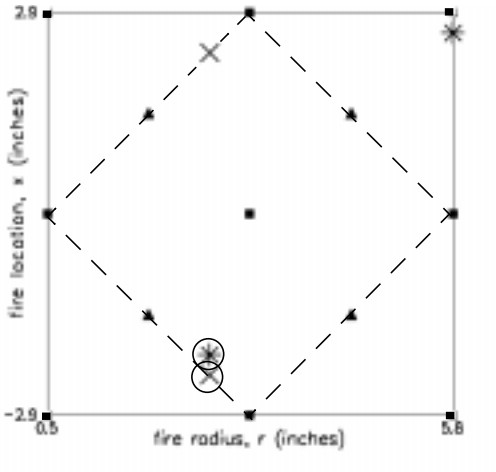

Figure 3 (Level 4)

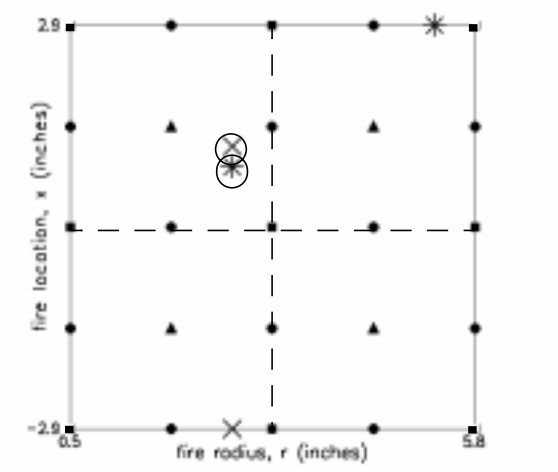

Figure 4 (Level 5)

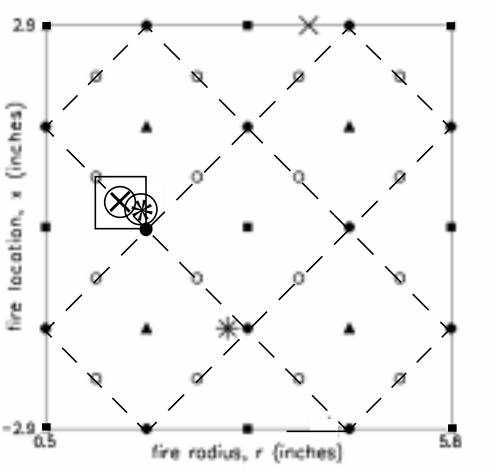

Figure 5 (Level 6)

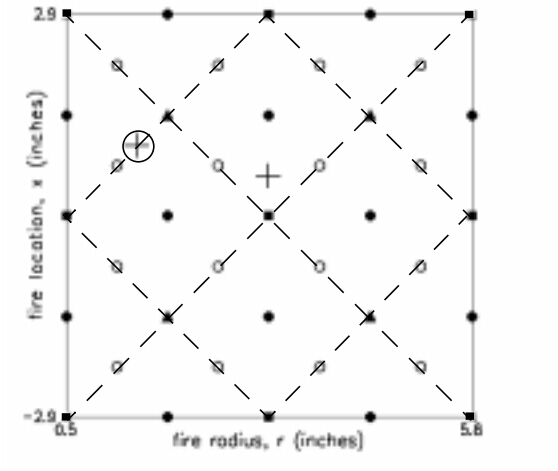

Figure 6 (Level 6, Interpolation II)

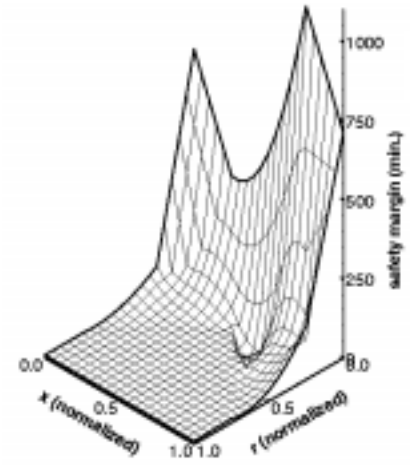

Figure 7 (Level 6 global response surface)

scale of parameter variations anticipated in the local search. Therefore, it is used as the initial "basis" model in the local optimization problem. Because objective function noise has been found to be effectively uncorrelated with model resolution (see *e.g.* [1]), any other model with sufficient local accuracy can serve as the "reference" model in the dual-model local schema. In light of its ability to replicate XLOOSE results globally, the X.5XLOOSE model is almost assured of possessing commensurate local accuracy. Therefore it will serve as the initial "reference" model. If during the process of local convergence meaningful divergence occurs between results of the basis and reference models, an upward switch in model resolution is enacted. Here an initial upgrade would be from XLOOSE to LOOSE tolerances for the basis model and from X.5XLOOSE to XLOOSE tolerances for the reference model. It turns out that the results of the X.5XLOOSE reference model effectively echo those of the XLOOSE basis model throughout the local convergence process. Therefore, no upward model switch is necessary and only XLOOSE results are presented in the following. (For research purposes a X.5XLOOSE/XXLOOSE initial reference/basis combination was tested and failed at the first decision juncture below, so the framework would immediately upgrade to the XLOOSE/X.5XLOOSE combination and reuse X.5XLOOSE samples from the initial unsuccessful step.)

The smallest "drawable" square about the dominant optimum identified in the global phase is shown in Figure 5. This square contains two existing sample points as vertices. Leveraging these two and performing 7 new FEVs attains a Level 3 interpolation over this subspace as shown in Figure 8. The local minimum on this updated interpolation surface occurs at the top edge of the subspace as indicated, with uncertainty of 1% of the subspace dimensions. A FEV is expended to determine if the indicated optimum is lower than the previous optimum and all new sample values, which it is, having an XLOOSE value of 2.854 minutes. According to the logic tree presented in [9], the indicated triangle adjoining the top edge of this subspace is populated next, leveraging one existing sample point and requiring 5 new FEVs to attain an updated quadratic representation of the objective function over this triangular subspace. The new local minimum over this subspace occurs at the × in the triangular subspace (with uncertainies in *r* and *x* of 1% of the lengths of its legs). The FEV value there is 2.607 minutes, which is the lowest confirmed minimum yet. Continuing on, the triangle is bisected and the "containing" triangle is windowed in on, as shown in Figure 8. Two new samples (FEVs) are required to fully populate it and the resulting response surface has a minimum at the indicated location. A FEV there yields a safety margin of 2.422 minutes, which is lower than the previous optimum. However, the circled sample point on the leg of the triangle has a lower value of 2.275 minutes, making **it** the optimum in this step and the lowest confirmed minimum yet. Further refinement about this point could be pursued, but the location of the global optimum has converged sufficiently at this point, having changed by only 0.7% in *r* and 0.2% in *x*, with < 1% being the set criterion here.

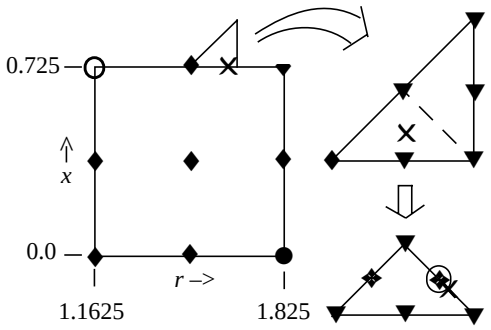

Figure 8

Finally, the XSTRICT model is run at the global minimum (circled sample point in Figure 8) to determine the asymptotic value of the global minimum (2.6182 min.) and verify that bias of the reference model remains relatively constant in the local phase (which it does, changing by less than 3% of the deepening of the minimum over the local phase). As a validation check on this framework, when using the fully converged XSTRICT model the global and local phases unfold as above, identifying the same global-minimum sample point (within uncertainty of +/-0.03% in *r* and *x*) as determined with the multimodel risk managing process illustrated above and costing about 1/10 in **total** with convergence studies.

6. References

[1] Romero, V. J., "Noise, Bias, Convergence, Resolution, Correlation, and Cost in Simulation and a Framework for Efficient Treatment of Uncertainty in Optimization Problems," Sandia National Laboratories report in preparation.

[2] Eldred, M.S., Outka, Bohnhoff, W.J., Witkowski, W.P., Romero, V.J., Ponslet, E.J., and Chen, K.S., "Optimization of Complex Mechanics Simulations with Object-Oriented Software Design," in *Computer Modeling and Simulation in Engineering*, Vol. 1 No. 3, August, 1996, pp. 323-352.

[3] Eldred, M.S., Hart, W.E., Bohnhoff, W.J., Romero, V.J., Hutchinson, S.A., and Salinger, A.G., "Utilizing Object-Oriented Design to Build Advanced Optimization Strategies with Generic Implementation," in the *Proceedings of the Sixth AIAA Multi-Disciplinary Optimization Symposium*, Belleview, WA, Sept. 4-6 1996.

[4] Romero, V.J., Painton, L.A., and Eldred, M.S., "Optimization Under Uncertainty: Accounting for uncertain component failure thresholds in finding the worst-case heating on a safing device," in preparation for submission to *Computer Modeling and Simulation in Engineering*

[5] Romero, V.J., Eldred, M.S., Bohnhoff, W.J., and Outka, D.E., "Application of Optimization to the Inverse Problem of Finding the Worst-Case Heating Configuration in a Fire," *Num. Mthds. in Thermal Problems*, Vol. IX, Part 2.

[6] P/THERMAL Analysis Package User Manuals, Release 2.6, March 1993, PDA Engineering, Costa Mesa, CA.

[7] Romero, V.J., "Treatment of Uncertain Emissivity in a Large Thermal Optimization Problem," in preparation for submission for the 33rd Joint National Heat Transfer Conference.

[8] Romero, V.J., and Bangston, S.D., "Finite-Element/Progressive-Lattice-Sampling Response Surface Methodology and Application to Benchmark Probability Quantification Problems," Sandia report *SAND98-0567* (March, 1998).

[9] Romero, V. J., "A Structured-Sampling Paradigm for Efficient Global Searching then Local Optimization with Noisy and Expensive Computer Models," Sandia National Laboratories report in preparation.